

Dysregulation of TGF- β activation contributes to pathogenesis in Marfan syndrome

Enid R. Neptune^{1,2}, Pamela A. Frischmeyer², Dan E. Arking², Loretha Myers², Tracie E. Bunton³, Barbara Gayraud⁴, Francesco Ramirez⁴, Lynn Y. Sakai⁵ & Harry C. Dietz^{2,6}

Published online 24 February 2003; doi:10.1038/ng1116

Marfan syndrome is an autosomal dominant disorder of connective tissue caused by mutations in fibrillin-1 (encoded by *FBN1* in humans and *Fbn1* in mice), a matrix component of extracellular microfibrils. A distinct subgroup of individuals with Marfan syndrome have distal airspace enlargement, historically described as emphysema, which frequently results in spontaneous lung rupture (pneumothorax; refs. 1–3). To investigate the pathogenesis of genetically imposed emphysema, we analyzed the lung phenotype of mice deficient in fibrillin-1, an accepted model of Marfan syndrome⁴. Lung abnormalities are evident in the immediate postnatal period and manifest as a developmental impairment of

distal alveolar septation. Aged mice deficient in fibrillin-1 develop destructive emphysema consistent with the view that early developmental perturbations can predispose to late-onset, seemingly acquired phenotypes. We show that mice deficient in fibrillin-1 have marked dysregulation of transforming growth factor- β (TGF- β) activation and signaling, resulting in apoptosis in the developing lung. Perinatal antagonism of TGF- β attenuates apoptosis and rescues alveolar septation *in vivo*. These data indicate that matrix sequestration of cytokines is crucial to their regulated activation and signaling and that perturbation of this function can contribute to the pathogenesis of disease.

Mice homozygous with respect to a centrally deleted *Fbn1* allele (*Fbn1*^{tm1Rmz}, herein called *Fbn1*^{mg Δ} ; ref. 4) die at postnatal day (PD) 7–10 from aortic dissection and rupture, recapitulating the vascular phenotype of Marfan syndrome⁴. At PD9, we observed a graded increase in distal airspace caliber in *Fbn1*^{+/mg Δ} and *Fbn1*^{mg Δ /mg Δ} mice compared with their wild-type (*Fbn1*^{+/+}) littermates (Fig. 1a,b). *Fbn1*^{mg Δ /mg Δ} mice had rare secondary alveolar septae (Fig. 1c), but their proximal airway caliber and vasculature appeared grossly normal. There was no inflammation or overt tissue damage. Calculation of mean linear intercepts (L_m ; ref. 5), a measure of the distance between alveolar structures, at PD1, PD4 and PD9 showed progressive distal airspace enlargement in the mutant mice, apparent from PD1 (Fig. 1a,b). Ratios of lung weight to body weight at PD5 were consistent in mice of all three genotypes (data not shown), arguing against overt lung hypoplasia. Thus, the early lung phenotype associated with deficiency in fibrillin-1 is most consistent with a

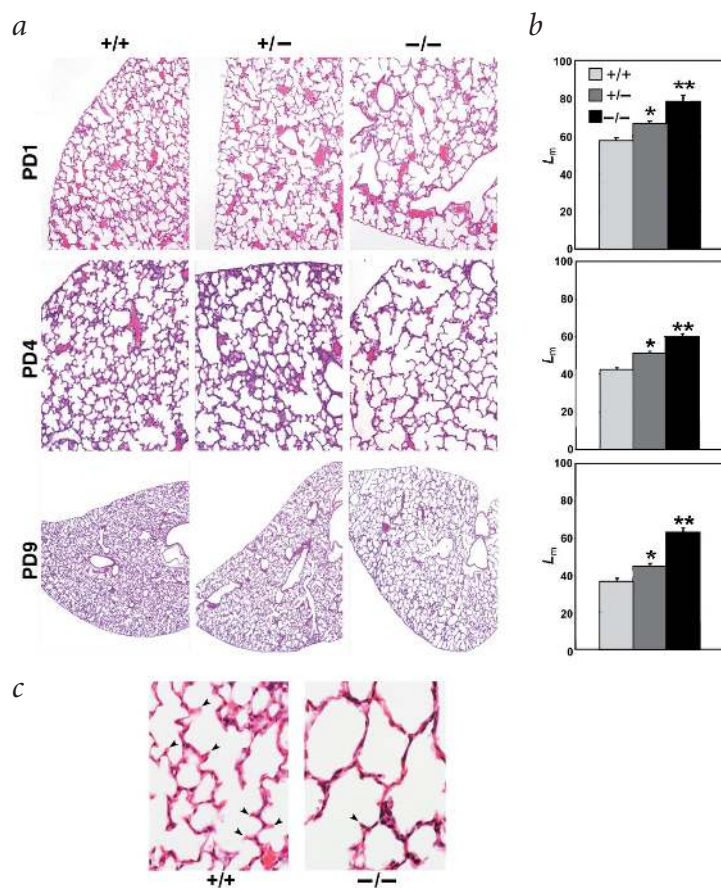


Fig. 1 Lung histopathology and morphometry of mice deficient in fibrillin-1. **a**, Lung sections from wild-type (+/+), *Fbn1*^{mg Δ /+} (+/-) and *Fbn1*^{mg Δ /mg Δ} (-/-) littermates at PD1, PD4 and PD9. A marked, progressive increase in distal airspace caliber is evident at all time points in *Fbn1*^{mg Δ /+} and *Fbn1*^{mg Δ /mg Δ} mice compared with wild-type littermates. Magnification: $\times 20$, except for PD9, $\times 2.5$. **b**, Lung morphometry at PD1, PD4 and PD9. The mean linear intercept (L_m), a measure of distal airspace enlargement, was calculated at the noted postnatal stages. Single asterisk indicates $P < 0.001$ compared with wild-type value, and double asterisk indicates $P < 0.001$ compared with heterozygote value. **c**, High-power magnification of lung sections of PD9 wild-type and *Fbn1*^{mg Δ /mg Δ} mice. Arrowheads indicate alveolar septal tips. Magnification: $\times 60$.

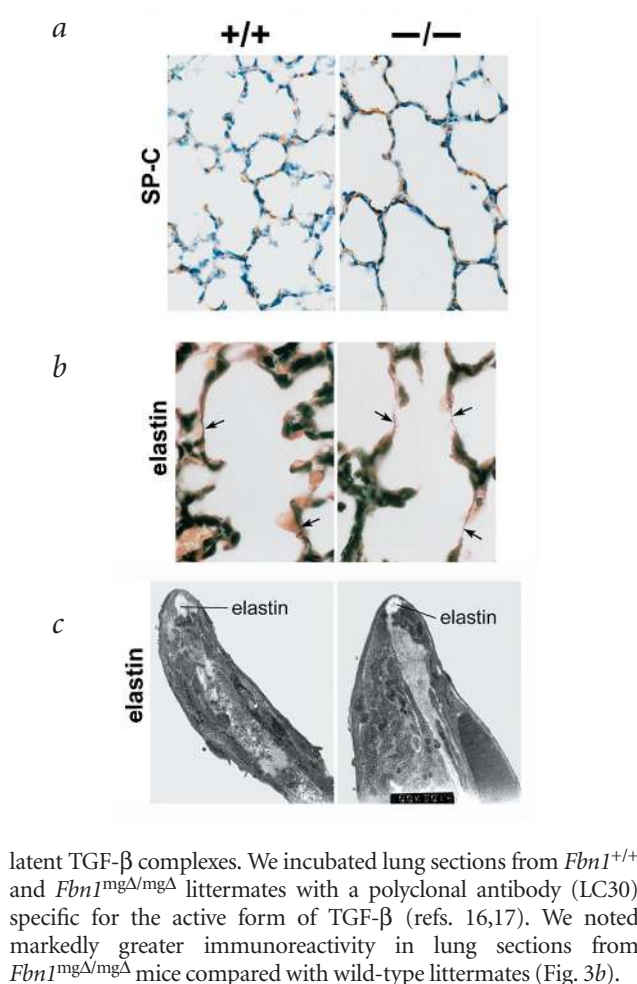
¹Division of Pulmonary and Critical Care Medicine and ²Institute of Genetic Medicine, Johns Hopkins University School of Medicine, Baltimore, Maryland 21205, USA. ³Department of Safety Assessment, Dupont Pharmaceuticals Company, Newark, Delaware 19714, USA. ⁴Hospital for Special Surgery, New York, New York 10021, USA. ⁵Shriners Hospital, Portland, Oregon 97201, USA. ⁶Howard Hughes Medical Institute, Johns Hopkins University School of Medicine, Baltimore, Maryland 21205, USA. Correspondence should be addressed to H.C.D. (e-mail: hdietz@jhmi.edu).

Fig. 2 Cell differentiation and elastin deposition in the lungs of mice deficient in fibrillin-1. **a**, Lung sections from PD7 wild-type (+/+) and *Fbn1*^{mgΔ/mgΔ} (–/–) mice were stained for surfactant protein C (SP-C). Magnification: ×20. **b,c**, Lung sections from PD9 wild-type (+/+) and *Fbn1*^{mgΔ/mgΔ} (–/–) mice were stained for elastin using a modified Hart's stain (**b**) and subjected to ultrastructural analysis (**c**). Arrows indicate elastin in the alveolar walls. Magnification: **b**, ×100 (oil); **c**, ×8800.

developmental perturbation of distal alveolar septation and not simple mechanical failure of a structurally deficient tissue, as was previously inferred.

Defects in distal airspace development can result from altered airway cell differentiation⁶. Using antibodies specific for surfactant protein C (a marker of differentiated alveolar type II cells), thyroid transcription factor 1 (a marker of distal airway and alveolar epithelial cells) and clara-cell-specific protein (a marker of non-ciliated distal airway cells), we found that all cell types were appropriately represented in the lungs of *Fbn1*^{mgΔ/mgΔ} mice (Fig. 2a and data not shown). During alveologensis, tropoelastin is deposited by smooth muscle cells and plausibly has a spatially instructive role for septation^{7–10}. Immunostaining with α-smooth muscle actin showed intact smooth muscle cell differentiation and distribution in the mutant lung (data not shown), and we observed preserved elastin deposition and localization to the tips of primordial septae (Fig. 2b,c). Taken together, these data suggest that abnormalities in cellular differentiation or elastin metabolism do not contribute considerably to the lung phenotype in *Fbn1*^{mgΔ/mgΔ} mice.

The fibrillins and latent TGF-β-binding proteins (LTBPs) constitute a family of structurally related proteins (Fig. 3a). One function of LTBPs may be to target latent TGF-β complexes to the extracellular matrix, but the connective tissue ligands for the LTBPs have yet to be fully elucidated^{11,12}. Because LTBP-1 has been immunolocalized to microfibrils containing fibrillin-1 and because LTBP-1 and LTBP-4 interact with fibrillin-1 (refs. 13–15), we hypothesized that loss of microfibrils might affect targeting and sequestration of



latent TGF-β complexes. We incubated lung sections from *Fbn1*^{+/+} and *Fbn1*^{mgΔ/mgΔ} littermates with a polyclonal antibody (LC30) specific for the active form of TGF-β (refs. 16,17). We noted markedly greater immunoreactivity in lung sections from *Fbn1*^{mgΔ/mgΔ} mice compared with wild-type littermates (Fig. 3b).

Fig. 3 Active TGF-β expression and signaling in lung tissue of mice deficient in fibrillin-1.

a, Homology between fibrillin-1 and LTBP-1. Domain types are shown at the bottom of the figure. Modified from ref. 24. **b**, Lung sections from wild-type (+/+) and *Fbn1*^{mgΔ/mgΔ} (–/–) littermates stained with a polyclonal antibody (LC30) specific for active TGF-β (upper panel; magnification: ×60, oil) and with an antibody specific for LAP-β1 (lower panel; magnification: ×40). **c**, Western blot of protein lysates from wild-type (+/+) and *Fbn1*^{mgΔ/mgΔ} (–/–) mouse lung, separated by 4–12% Bis-Tris gradient gels and probed with antibodies against LAP-β1 and β-actin. SLC, small latent complex of TGF-β1. (The SLC band corresponds to the predominant complex containing LAP-β1 present in the lung lysates.) **d**, Reporter transgene used to assay TGF-β signaling. **e**, Fluorescence micrographs from lungs of PD7 wild-type (+/+) and *Fbn1*^{mgΔ/mgΔ} (–/–) mice expressing the GFP transgene and of a wild-type non-transgenic mouse (ntg). **f**, Semiquantitative analysis of fluorescence intensity in the lungs of transgenic fibrillin-1-deficient and wild-type mice. Compared with wild-type mice (+/+), mean pixel intensity was 4 and 25 times greater, respectively, in *Fbn1*^{mgΔ/mgΔ} (+/–) and *Fbn1*^{mgΔ/mgΔ} (–/–) mice. Single asterisk indicates $P < 0.05$ compared with wild-type value, and double asterisk indicates $P < 0.001$ compared with wild-type value.

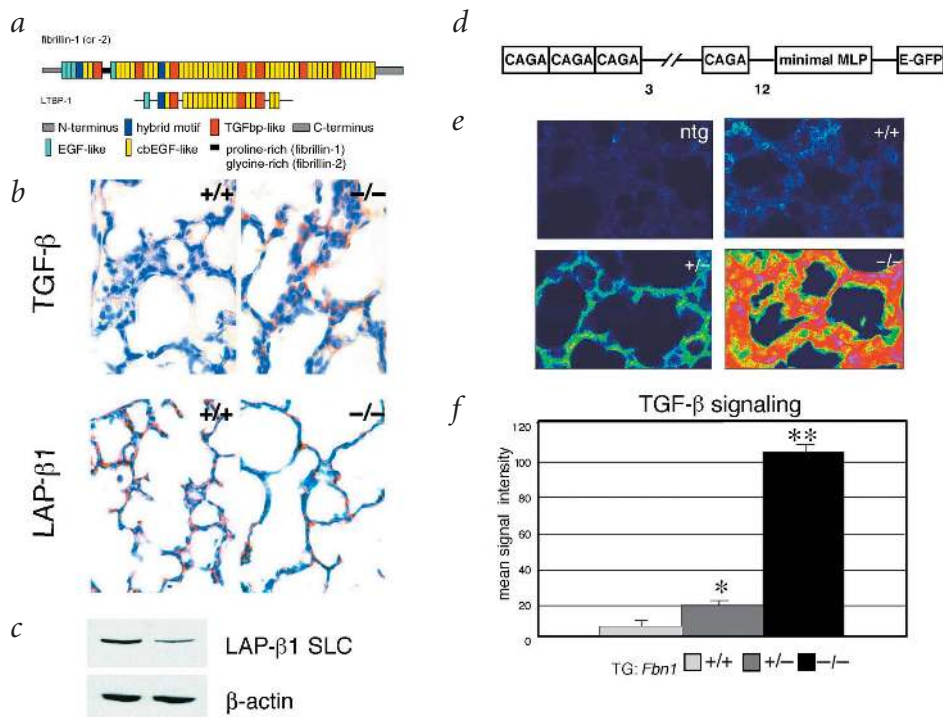


Fig. 4 Neutralizing antibody to TGF- β rescues lung maturation in mice deficient in fibrillin-1. **a**, Lung sections from PD7 wild-type (+/+), *Fbn1*^{mg Δ /+} (+/-) and *Fbn1*^{mg Δ /mg Δ} (-/-) mice treated *in utero* with TGF- β -neutralizing antibody (neu Ab) at the indicated doses. Magnification: $\times 20$. **b**, Improvement in distal lung caliber in wild-type (+/+), *Fbn1*^{mg Δ /+} (+/-) and *Fbn1*^{mg Δ /mg Δ} (-/-) mice confirmed by morphometry. Single asterisk indicates $P < 0.001$ compared with control value, and double asterisk indicates $P < 0.001$ compared with mice treated with 5 mg of TGF- β -neutralizing antibody (neu Ab) per kg body weight.

To determine whether this reflected greater TGF- β synthesis and secretion, we assessed the abundance of latency-associated peptide- $\beta 1$ (LAP- $\beta 1$), the processed N-terminal propeptide of TGF- $\beta 1$ that remains non-covalently linked to TGF- $\beta 1$ (termed the small latent complex) during secretion and matrix sequestration. We observed lower immunoreactivity for LAP- $\beta 1$ in the mutant lung (Fig. 3b,c), suggesting that the greater amount of active TGF- β in *Fbn1*^{mg Δ /mg Δ} mice reflects greater local activation rather than greater secretion. To assess TGF- β signaling *in vivo*, we introduced a reporter gene containing twelve tandem CAGA boxes (TGF- β -responsive promoter elements; ref. 18) upstream of a gene encoding green fluorescent protein (GFP) into the fibrillin-1-deficient background (Fig. 3d). Fluorescence micrographs (Fig. 3e,f) showed moderately enhanced signaling in *Fbn1*^{mg Δ /+} mice and markedly enhanced signaling in *Fbn1*^{mg Δ /mg Δ} mice (by factors of 4 and 25, respectively, relative to that observed in wild-type mice).

To determine whether enhanced TGF- β signaling contributed to the impairment in distal airspace septation, we administered a TGF- β -neutralizing antibody to late-gestation pregnant mice deficient in fibrillin-1 (from *Fbn1*^{mg Δ /+} matings). This antibody neutralizes the activity of TGF- β isoforms 1 and 2 both *in vivo* and *in vitro*^{19,20}. Histological analysis of PD7 pups showed a dose-dependent increase in septation in all genotypes, with the most pronounced effect seen in *Fbn1*^{mg Δ /mg Δ} mice (Fig. 4a,b). These data suggest that TGF- β is a physiologic inhibitor of alveolar septation in the mouse lung and underlies impairment of septation in mice deficient in fibrillin-1.

TGF- β can inhibit proliferation or stimulate apoptosis of lung epithelial cells²¹. We found that proliferation, as assessed by immunostaining with Ki67 and labeling with 5-bromo-2-deoxyuridine (BrdU), was preserved in the mutant lungs (Fig. 5a and data not shown). TUNEL staining showed greater apoptosis in the lungs of PD7 *Fbn1*^{mg Δ /mg Δ} mice (Fig. 5b). After treatment with TGF- β neutralizing antibody, TUNEL staining was lower in the mutant lung parenchyma with persistent staining at the periphery (Fig. 5c), similar to that of the untreated wild-type lung.

Because *Fbn1*^{mg Δ /mg Δ} mice die within the first two weeks of life, we examined the adult lung phenotype of *Fbn1*^{mgR/mgR} mice, an alternative model of Marfan syndrome. These mice harbor a hypomorphic *Fbn1* allele (*Fbn1*^{tm2Rmz}, herein called *Fbn1*^{mgR}) and die within the first 6–9 months of life owing to aortic rupture²². We observed more active TGF- β and impaired alveolar septation in *Fbn1*^{mgR/mgR} mice at 2 weeks of age (Fig. 6a,b), similar to findings in *Fbn1*^{mg Δ /mg Δ} mice. By 6 months of age, *Fbn1*^{mgR/mgR} mice developed marked airspace dilatation associated with destructive changes, peribronchiolar inflammation

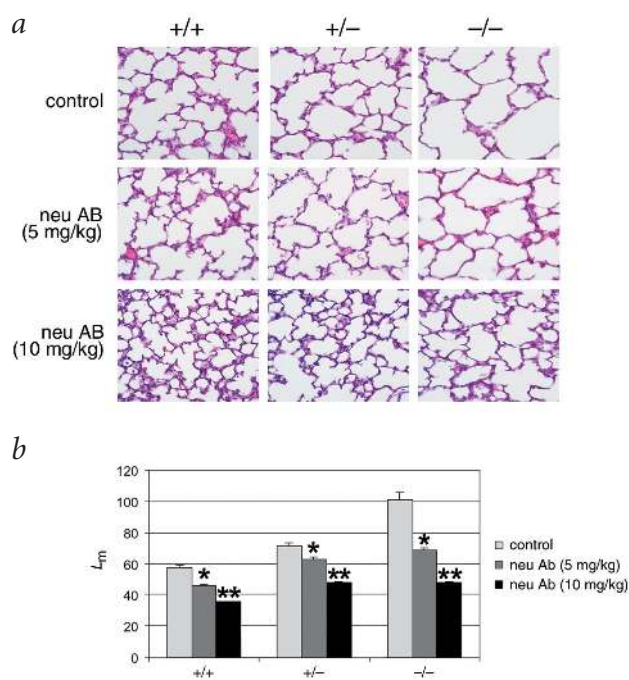


(Fig. 6b,c) and greater expression of matrix metalloproteases (data not shown), thus fully recapitulating the pathologic findings of human emphysema.

Our current mechanistic hypothesis is that deficiency in fibrillin-1 alters or precludes matrix sequestration of the large latent complex of TGF- β and that this event renders the cytokine more prone to or accessible for activation. These findings support three important new paradigms. First, structural matrix elements can also serve crucial regulatory roles in cytokine activation and signaling, and perturbation of this process can contribute to disease pathogenesis. Second, these data provide a direct link between TGF- β activation and signaling and regulation of distal alveolar septation. They also further the view that

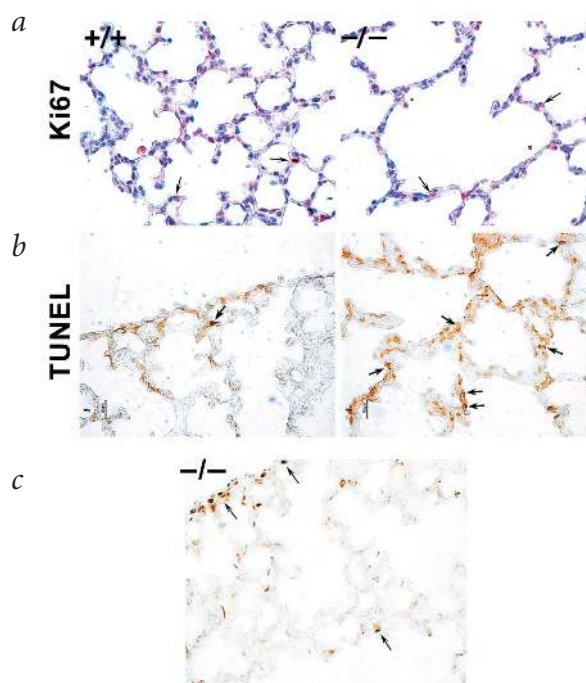


Fig. 5 Mice deficient in fibrillin-1 have preserved lung cell proliferation but greater apoptosis. **a**, Lung sections from PD7 wild-type (+/+) and *Fbn1*^{mg Δ /mg Δ} (-/-) mice immunostained for Ki67, a marker of proliferation. Arrows indicate representative cells with positive staining. **b**, TUNEL stain of lung sections from PD7 wild-type (+/+) and *Fbn1*^{mg Δ /mg Δ} (-/-) mice. In wild-type mice, TUNEL staining was restricted to the pleural surface of the lungs. Scale bar: 10 μ m. **c**, TUNEL stain of lung section from a PD7 *Fbn1*^{mg Δ /mg Δ} (-/-) mouse treated prenatally with TGF- β -neutralizing antibody. Arrows in **b** and **c** indicate representative cells with positive TUNEL staining.

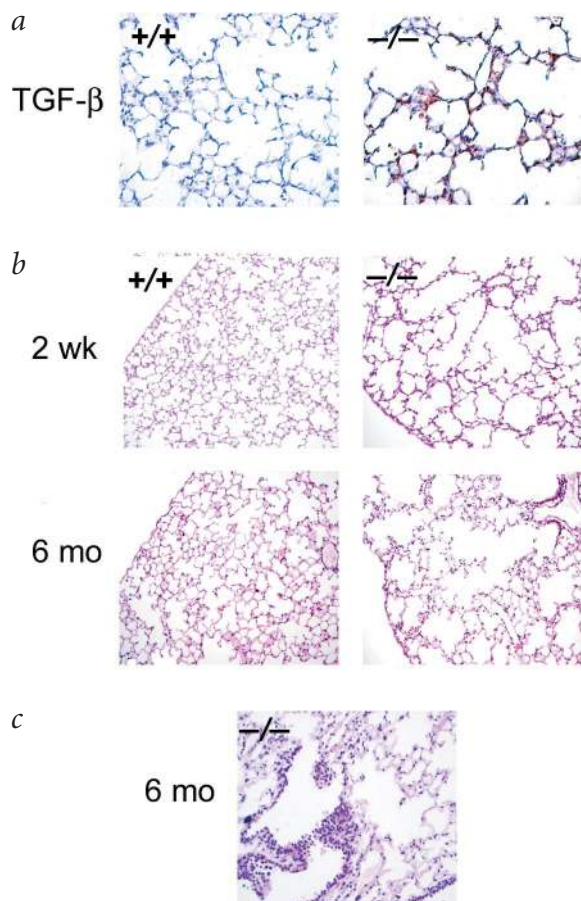


Fig. 6 Lung phenotype of wild-type (+/+) and *Fbn1*^{mgR/mgR} (-/-) mice. **a**, Immunostaining for active TGF-β is enhanced in 2-wk-old mutant mice compared with wild-type littermates. Magnification: ×20. **b**, Lung histology of wild-type (+/+) and *Fbn1*^{mgR/mgR} (-/-) mice at 2 wk (upper panel) and 6 mo (lower panel). Magnification: ×20. **c**, Higher-power magnification of lung from a 6-mo-old mutant mouse shows peribronchiolar inflammation. Magnification: ×40.

protein C (provided by J. Whitsett), thyroid transcription factor 1 (DAKO Systems), LAP-β1 (R&D Systems) or Ki67 (Santa Cruz Biotechnology). We washed the sections in phosphate-buffered saline and incubated them with secondary antibody reagents according to the Vectastain Elite protocol for peroxidase labeling (Vector Laboratories). We then applied diaminobenzidine chromogen (Sigma) as a substrate, counterstained the slides with hematoxylin and mounted them with Crystallmount (Biomed). Specificity was determined by omitting the primary antibody and running negative controls in parallel. Positive immunoreactivity was indicated by the intensity and distribution of staining.

Generation of CAGA12/GFP transgenic mice. We constructed the CAGA/GFP transgene vector by ligating a fragment of the pEGFP-C1 C-Terminal Protein Fusion Vector (CLONtech Laboratories) containing the EGFP cassette to a fragment of the (CAGA)12MLPLuc plasmid¹⁸ containing an upstream CAGA(12) sequence without the luciferase reporter fragment. We microinjected this transgene into BL6/SJL F2 embryos and transferred them into pseudopregnant mice. We identified four founders that possessed the transgene and backcrossed one of them into C57BL/6 to establish the line used in this study. We genotyped the mice by Southern blotting, which also verified equivalent copy number of the transgene between littermates of various *Fbn1* genotype (data not shown), and maintained them as heterozygotes for subsequent crosses.

Electron microscopy. We euthanized two mice of each genotype at PD4 as described above. We collected lungs and inflated them at 25 cm H₂O with 3% cold glutaraldehyde in 0.1 M sodium cacodylate buffer. We postfixed the lungs with 1% osmium tetroxide in 0.1 M sodium cacodylate buffer. We prepared, sectioned and analyzed the tissues as previously described²³.

Confocal fluorescence microscopy. Images were acquired with the Noran Oz Confocal Laser Scanning Microscope System using Intervention Software (version 6.5) on a Silicon Graphics O2 platform. We used a Krypton-Argon laser (Omnichrome, series 43) exciting at 488 wavelengths to obtain optical sections. We used narrow-band emission filters (525 nm) to eliminate channel cross-talk and a 10-μm mixed slit to obtain 0.5-μm Z-plane sections (as determined by full width, half-maximum intensity values). Slides were imaged with a ×60 oil-immersion planar apochromatic objective lens (n.a. 1.4) through an Olympus IX-50 inverted microscope. Images were placed on view with the exponential colormap. For each genotype, we measured pixel value intensity (0–255) with a two-dimensional segmentation tool. We calculated an average of pixel values from multiple fields and a standard deviation after subtracting the background (non-transgenic) value. We carried out this analysis on at least three mice per genotype with consistent results.

Lung morphometry. For the quantitative assessment of distal airspace enlargement, we used the mean linear intercept (L_m) value⁶. We fixed, inflated and paraffin-embedded lungs as described above. We cut several 5-μm sagittal sections of each lung and stained them with hematoxylin and eosin. To determine L_m , we evaluated at least 10 histological fields in both lungs of 5 or more mice. We grouped mice of the same genotype and combined the morphometry data to generate a 95% confidence interval for each genotype.

TGF-β-neutralizing antibody treatment. On embryonic days 17 and 19, we injected female heterozygotes (*Fbn1*^{mgR/+}) pregnant from timed matings with male heterozygotes intraperitoneally with TGF-β-neutralizing antibody (R&D Systems). The antibody was diluted into phosphate-buffered saline (pH 7.4) at the noted concentrations and administered to the pregnant female in a volume of 500 μl. For control experiments, we administered rabbit IgG (Sigma) at the highest dose (10 mg per kg body weight) in a similar fashion.

early developmental perturbations can predispose to late-onset and apparently acquired phenotypes such as emphysema. Third, this pathogenetic mechanism may underlie other manifestations of Marfan syndrome that are not easily reconciled by loss of mechanical tissue integrity, including myxomatous changes of valve leaflets and bone overgrowth. Selective pathologies may be amenable to treatments that attenuate excessive cytokine activity.

Methods

Mice. Targeted disruption of *Fbn1* has been described^{4,5}. We determined genotypes of all offspring by Southern-blot analysis of genomic DNA. For morphological studies, we examined 5–8 mice of each relevant genotype at each designated time point. Histology was consistent among all wild-type mice, and the abnormalities seen in mice deficient in fibrillin-1 were observed in all sections (both lungs per mouse, ≥10 fields per lung) from mice examined within a given genotype. All mouse protocols were approved by the Animal Care and Use Committee of Johns Hopkins University School of Medicine.

Tissue preparation. After mice were euthanized with metoflurane, we collected lungs en bloc and inflated them through the trachea with 4% paraformaldehyde at a pressure of 25 cm H₂O for 30 min. We fixed lungs overnight in 4% paraformaldehyde and embedded them in paraffin. For GFP analysis, the lungs were similarly inflated and fixed, but we subsequently infused them with 18% sucrose, froze them in optimal cutting temperature compound and sectioned them.

Microscopic examination. We prepared tissue slides and stained them with either hematoxylin and eosin or a modified Hart's stain for elastin. For immunohistochemistry, we removed paraffin from 5-μm sections of paraffin-embedded tissue with xylene, rehydrated sections in an ethanol series, washed them and then incubated them with specific primary antibodies recognizing active TGF-β (provided by K. Flanders), surfactant

Western blotting of lung lysates. We collected lungs from PD7 mice, homogenized them and lysed them in RIPA buffer. After centrifugation, we recovered the supernatants and quantified the protein using the Biorad RC/DC Kit (Biorad). We mixed equivalent amounts of lysates from wild-type and mutant mice with sample buffer and separated them on a NuPAGE 4–12% Bis-Tris gel (Invitrogen). The samples were electrophoretically transferred to nitrocellulose and blocked overnight at 4 °C in phosphate-buffered saline containing 5% nonfat dry milk, 0.1% Tween 20 and sodium azide. We incubated the membranes overnight at 4 °C with primary antibodies against LAP-β1 (R&D Systems) or against β-actin (from Santa Cruz Biotechnology) at 1:2,000 dilution. After washing the membranes, we applied horseradish peroxidase-conjugated secondary antibodies against goat (for LAP-β1) or against rabbit (for β-actin) for 1 h at room temperature. We used enhanced chemiluminescence to detect labeled antigen. This analysis was repeated on multiple lysates with identical results.

BrdU and TUNEL labeling. For BrdU labeling, we injected PD5 pups intraperitoneally with BrdU stock solution following the Zymed protocol. After 3 h, we euthanized mice and collected the lungs, fixed them in 4% paraformaldehyde, sectioned them, embedded them in paraffin and processed them accordingly. For TUNEL labeling, we prepared paraformaldehyde-fixed, paraffin-embedded sections and labeled them according to the In Situ Cell Death Detection Kit (Roche) protocol.

Acknowledgments

We thank J. Gauthier for providing reagents, D. Valle for helpful comments about the manuscript, M. Barcellos-Hoff for advice about the use of TGF-β antibodies, M. Dellanoy for help with confocal imaging and members of H.C.D.'s laboratory for their support and advice. This work was supported by Robert Wood Johnson Foundation (to E.R.N.), Howard Hughes Medical Institute (to H.C.D.), US National Institutes of Health grants (to E.R.N., H.C.D. and F.R.), the Michael Murray fund from the National Marfan Foundation (to H.C.D.), Smilow Foundation (to H.C.D.) and Dr. Amy and James Elster Research Fund (to F.R.).

Competing interests statement

The authors declare that they have no competing financial interests.

Received 13 September 2002; accepted 30 January 2003.

1. Dwyer, E.M. & Troncale, F. Spontaneous pneumothorax and pulmonary disease in the Marfan syndrome. *Ann. Intern. Med.* **62**, 1285–1292 (1965).
2. Hall, J.R., Pyeritz, R.E., Dudgeon, D.L. & Haller, J.A., Jr. Pneumothorax in the Marfan syndrome: prevalence and therapy. *Ann. Thorac. Surg.* **37**, 500–504 (1984).

3. Wood, J.R., Bellamy, D., Child, A.H. & Citron, K.M. Pulmonary disease in patients with Marfan syndrome. *Thorax* **39**, 780–784 (1984).
4. Pereira, L. et al. Targeting of the gene encoding fibrillin-1 recapitulates the vascular aspect of Marfan syndrome. *Nat. Genet.* **17**, 218–222 (1997).
5. Thurlbeck, W.M. Measurement of pulmonary emphysema. *Am. Rev. Respir. Dis.* **95**, 752–764 (1967).
6. Zhou, L., Lim, L., Costa, R.H. & Whitsett, J.A. Thyroid transcription factor-1, hepatocyte nuclear factor-3β, surfactant protein B, C, and Clara cell secretory protein in developing mouse lung. *J. Histochem. Cytochem.* **44**, 1183–1193 (1996).
7. Bostrom, H. et al. PDGF-A signaling is a critical event in lung alveolar myofibroblast development and alveogenesis. *Cell* **85**, 863–873 (1996).
8. Nakamura, T. et al. Fibulin-5/DANCE is essential for elastogenesis *in vivo*. *Nature* **415**, 171–175 (2002).
9. Weinstein, M., Xu, X., Ohyama, K. & Deng, C.X. FGFR-3 and FGFR-4 function cooperatively to direct alveogenesis in the murine lung. *Development* **125**, 3615–3623 (1998).
10. Wendel, D.P., Taylor, D.G., Albertine, K.H., Keating, M.T. & Li, D.Y. Impaired distal airway development in mice lacking elastin. *Am. J. Respir. Cell Mol. Biol.* **23**, 320–326 (2000).
11. Taipale, J., Saharinen, J., Hedman, K. & Keski-Oja, J. Latent transforming growth factor-β 1 and its binding protein are components of extracellular matrix microfibrils. *J. Histochem. Cytochem.* **44**, 875–889 (1996).
12. Unsold, C., Hyytiäinen, M., Bruckner-Tuderman, L. & Keski-Oja, J. Latent TGF-β binding protein LTBP-1 contains three potential extracellular matrix interacting domains. *J. Cell. Sci.* **114**, 187–197 (2001).
13. Dallas, S.L., Miyazono, K., Skerry, T.M., Mundy, G.R. & Bonewald, L.F. Dual role for the latent transforming growth factor-β binding protein in storage of latent TGF-β in the extracellular matrix and as a structural matrix protein. *J. Cell Biol.* **131**, 539–549 (1995).
14. Dallas, S.L. et al. Role of the latent transforming growth factor-β binding protein 1 in fibrillin-containing microfibrils in bone cells *in vitro* and *in vivo*. *J. Bone Miner. Res.* **15**, 68–81 (2000).
15. Isogai, Z. et al. Latent transforming growth factor-β binding protein 1 interacts with fibrillin and is a microfibril-associated protein. *J. Biol. Chem.* **278**, 2750–2757 (2003).
16. Barcellos-Hoff, M.H. et al. Immunohistochemical detection of active transforming growth factor-β *in situ* using engineered tissue. *Am. J. Pathol.* **147**, 1228–1237 (1995).
17. Flanders, K.C. et al. Transforming growth factor-β 1: histochemical localization with antibodies to different epitopes. *J. Cell Biol.* **108**, 653–660 (1989).
18. Dennler, S. et al. Direct binding of Smad3 and Smad4 to critical TGFβ-inducible elements in the promoter of human plasminogen activator inhibitor-type 1 gene. *EMBO J.* **17**, 3091–3100 (1998).
19. Tomita, H. et al. Early induction of transforming growth factor-β via angiotensin II type 1 receptors contributes to cardiac fibrosis induced by long-term blockade of nitric oxide synthesis in rats. *Hypertension* **32**, 273–279 (1998).
20. Yamamoto, T., Takagawa, S., Katayama, I. & Nishioka, K. Anti-sclerotic effect of transforming growth factor-β antibody in a mouse model of bleomycin-induced scleroderma. *Clin. Immunol.* **92**, 6–13 (1999).
21. Moustakas, A., Pardali, K., Gaal, A. & Heldin, C.H. Mechanisms of TGF-β signaling in regulation of cell growth and differentiation. *Immunol. Lett.* **82**, 85–91 (2002).
22. Pereira, L. et al. Pathogenetic sequence for aneurysm revealed in mice underexpressing fibrillin-1. *Proc. Natl. Acad. Sci. USA* **96**, 3819–3823 (1999).
23. Bunton, T.E. et al. Phenotypic alteration of vascular smooth muscle cells precedes elastolysis in a mouse model of Marfan syndrome. *Circ. Res.* **88**, 37–43 (2001).
24. Nijbroek, G. et al. Fifteen novel *FBN1* mutations causing Marfan syndrome detected by heteroduplex analysis of genomic amplicons. *Am. J. Hum. Genet.* **57**, 8–21 (1995).